Hemidesmosome integrity protects the colon against colitis and colorectal cancer

Adèle de Arcangelis, Hussein Hamade, Fabien Alpy, Sylvain Normand, Emilie Bruyère, Olivier Lefebvre, Agnès Méchine-Neuville, Stéphanie Siebert, Véronique Pfister, Patricia Lepage, et al.

OPEN ACCESS

ORIGINAL ARTICLE

Hemidesmosome integrity protects the colon against colitis and colorectal cancer

Adèle De Arcangelis,[1,2,3,4] Hussein Hamade,[1,2,3,4,5] Fabien Alpy,[2,3,4,6,7] Sylvain Normand,[8] Emilie Bruyère,[9] Olivier Lefebvre,[4,6,10,11] Agnès Méchine-Neuville,[6,12,13] Stéphanie Siebert,[1,2,3,4] Véronique Pfister,[1,2,3,4] Patricia Lepage,[14] Patrice Laquerriere,[4,15] Doulaye Dembele,[1,2,3,4] Anne Delanoye-Crespin,[8] Sophie Rodius,[1,2,3,4,16] Sylvie Robine,[17,18] Michèle Kedinger,[4,6] Isabelle Van Seuningen,[9] Patricia Simon-Assmann,[4,6,10,11] Mathias Chamaillard,[8] Michel Labouesse,[1,2,3,4,19] Elisabeth Georges-Labouesse[1,2,3,4]

► Additional material is published online only. To view please visit the journal online (http://dx.doi.org/10.1136/gutjnl-2015-310847).

For numbered affiliations see end of article.

Correspondence to
Adèle De Arcangelis, IGBMC, 1 rue Laurent Fries, F-67400 Illkirch, France; adele@igbmc.frMichel Labouesse, UMR7622, IBPS, UPMC, 9 quai Saint-Bernard, F-75005 Paris, France; michel.labouesse@upmc.fr

This work is a warm tribute to Elisabeth who initiated this study and supervised it until passing away in July 2012., ADA and HH contributed equally to the present study.

Received 4 October 2015
Revised 12 May 2016
Accepted 30 May 2016
Published Online First 1 July 2016

ABSTRACT

Objective Epidemiological and clinical data indicate that patients suffering from IBD with long-standing colitis display a higher risk to develop colorectal high-grade dysplasia. Whereas carcinoma invasion and metastasis rely on basement membrane (BM) disruption, experimental evidence is lacking regarding the potential contribution of epithelial cell/BM anchorage on inflammation onset and subsequent neoplastic transformation of inflammatory lesions. Herein, we analyse the role of the α6β4 integrin receptor found in hemidesmosomes that attach intestinal epithelial cells (IECs) to the laminin-containing BM.

Design We developed new mouse models inducing IEC-specific ablation of α6 integrin either during development ($\alpha6^{\Delta IEC}$) or in adults ($\alpha6^{\Delta IEC\text{-}TAM}$).

Results Strikingly, all $\alpha6^{\Delta IEC}$ mutant mice spontaneously developed long-standing colitis, which degenerated overtime into infiltrating adenocarcinoma. The sequence of events leading to disease onset entails hemidesmosome disruption, BM detachment, IL-18 overproduction by IECs, hyperplasia and enhanced intestinal permeability. Likewise, IEC-specific ablation of α6 integrin induced in adult mice ($\alpha6^{\Delta IEC\text{-}TAM}$) resulted in fully penetrant colitis and tumour progression. Whereas broad-spectrum antibiotic treatment lowered tissue pathology and IL-1β secretion from infiltrating myeloid cells, it failed to reduce Th1 and Th17 response. Interestingly, while the initial intestinal inflammation occurred independently of the adaptive immune system, tumourigenesis required B and T lymphocyte activation.

Conclusions We provide for the first time evidence that loss of IECs/BM interactions triggered by hemidesmosome disruption initiates the development of inflammatory lesions that progress into high-grade dysplasia and carcinoma. Colorectal neoplasia in our mouse models resemble that seen in patients with IBD, making them highly attractive for discovering more efficient therapies.

Significance of this study

What is already known on this subject?

- Loss of the major laminin receptor in hemidesmosomes, namely the α6β4 integrin, leads to severe skin barrier defects in mice and humans.
- Genome-wide association studies hint at a potential implication of basement membrane (BM) laminins in predisposition to IBD and colorectal cancer (CRC). Laminin expression and distribution are altered in patients with IBD and CRC.
- Numerous cytokines have been shown to influence disease progression, along with interleukin-18 (IL-18), which contributes to the regulation of goblet cells (GCs) and to the maintenance of gut barrier function.
- Tumour immunosurveillance is thought to be impaired in patients with IBD with long-standing extensive colitis.

What are the new findings?

- Mice carrying intestinal epithelial cell (IEC)-specific loss of α6 integrin develop fully penetrant colitis which spontaneously degenerates into carcinoma of the rectal mucosa that is the most intensely subject to environmental stress.
- The onset of colitis is preceded by defective anchorage of the mutant IECs to the BM due to loss of hemidesmosomes, which results in a strong activation of caspase-1 leading to the secretion of IL-18, known to regulate GC functions.
- Colitis is independent of T and B cell activation, but relies on increased epithelial secretion of IL-18 and important accumulation of intestinal $CD11b^{+}$ myeloid cells that oversecrete IL-1β as a consequence of bacterial translocation through the defective mucus barrier. Broad spectrum antibiotic treatment partially improves colitis.
- Risk of developing dysplasia leading to CRC relies on the activation of the adaptive immune response.

INTRODUCTION

Intestinal homeostasis depends on a fine symbiosis among the epithelium, the immune system and the commensal bacteria present in the lumen. The polarised intestinal epithelium, with its mucus layer

To cite: De Arcangelis A, Hamade H, Alpy F, *et al*. *Gut* 2017;**66**:1748–1760.

Significance of this study

How might it impact on clinical practice in the foreseeable future?

- Our findings reveal that the epithelial barrier/BM connection plays a critical role in the maintenance of intestinal integrity and homeostasis, by contributing to the formation of an efficient epithelial and mucus barrier. Improving weakened epithelial/BM interactions and restoring a functional mucus barrier by targeting epithelial IL-18/IL-18R signalling and by using diet that reduces the mechanical stress may represent novel therapeutic avenues in IBD.
- Our results highlight also the crucial role of the IL-1 family of cytokines during progression of the inflammatory lesions into colorectal adenocarcinomas. This work suggests that tumour progression in IBD could be improved or slowed down by reducing the inflammatory context mediated by IL-1/IL-1R with specific drugs or neutralising antibodies.

on its apical side and the basement membrane (BM) on its basal side, plays a central role in establishing the barrier function essential for symbiotic relationship with the gut microbiota.[1–3] Compromising with intestinal homeostasis can lead to pathologies, such as IBD. IBD are relapsing-remitting illnesses, which can evolve into colorectal cancer (CRC) among patients with long-standing extensive colitis.[4–6] Immune system dysregulation, mucus layer alterations, aberrant endoplasmic reticulum stress response and abnormal cell–cell junctions have been linked to IBD development.[1 7 8] However, how interactions mediated by integrin receptors between the epithelium and its underlying BM contribute to maintain intestinal homeostasis has been largely overlooked.[9]

Major players of these interactions are the hemidesmosomes, which consist in specific junctions present at the base of all intestinal epithelial cells (IECs) where the α6β4 integrin interconnects the BM laminin-332 to keratin filaments through the cytoplasmic-linker protein plectin.[10 11] Interestingly, several genetic studies have indirectly linked BM laminins and their integrin receptors to several intestinal pathologies. First, genome-wide-association studies have identified the *LAMB1* (encoding the laminin β1 chain; association probability between 10^{-6} and 3×10^{-8}) and *LAMC1* (encoding the laminin γ1 chain; association probability 10^{-7}) loci as susceptibility loci predisposing to IBD[12 13] and CRC,[14] respectively. Foremost, intestinal erosions reminiscent to IBD are found in patients suffering from skin disorders that are caused by hemidesmosome defects.[15] Conversely, patients with IBD may develop skin lesions such as psoriasis,[16] a skin inflammatory defect observed in mice lacking α6 integrin in basal keratinocytes.[17]

To investigate the potential role of α6β4 integrin in intestinal homeostasis, we generated two mouse models carrying either a targeted deletion of the integrin α6 gene *(Itga6)* in IECs, named the $\alpha6^{\Delta IEC}$ line or a tamoxifen (TAM)-inducible deletion, named the $\alpha6^{\Delta IEC\text{-}TAM}$ line. Strikingly, all $\alpha6^{\Delta IEC}$ and $\alpha6^{\Delta IEC\text{-}TAM}$ mutant animals developed long-standing extensive colitis. Foremost, inflammatory lesions spontaneously and progressively degenerated into infiltrating colorectal adenocarcinomas in $\alpha6^{\Delta IEC}$ mice, as well as in the $\alpha6^{\Delta IEC\text{-}TAM}$ model. Characterisation of both models demonstrates the central protective role of the epithelial cell/BM connection in preserving intestinal homeostasis and in preventing the risk of colitis-associated cancer.

RESULTS

Epithelial-specific genetic ablation of *Itga6* affects intestinal hemidesmosomes

To assay the role of α6 integrin in intestinal homeostasis, we first induced a complete deletion of *Itga6* in IECs using the Cre-lox approach[18] ($\alpha6^{\Delta IEC}$; figure 1A and online supplementary figure S1). The resulting animals displayed abnormally loose and viscous stools, and frequently developed a rectal prolapse (figure 1B). To determine whether this phenotype was linked to hemidesmosome alterations, we examined the β4 integrin chain, the α6 hemidesmosome heterodimerising partner and found that both chains were removed from IECs at all stages examined (see figure 1C–E and online supplementary figure S2A, B). By contrast, epithelial expression of integrin β1, which can also heterodimerise with other α chains, did not vary (see online supplementary figure S2C), confirming that defects observed in these mice originated from a loss of the α6β4 integrin in the epithelium.

We next tested if *Itga6* depletion in IECs impaired the assembly of the hemidesmosome component plectin and subsequently of keratins 8/18 (K8/18). Plectin, which interacts with the β4 integrin cytoplasmic domain, was detected in hemidesmosomal basal patches and at the apical membrane of control IECs (figure 1F). In $\alpha6^{\Delta IEC}$ mice, plectin staining was strongly reduced basally but not apically; loss of basal plectin was already observed in late $\alpha6^{\Delta IEC}$ embryos (see figure 1F and online supplementary figure S2D). Moreover, the K8/18 intermediate filament dimers, which normally are concentrated in the plectin patches basally, were diffusely distributed throughout the cytoplasm (figure 1G). As a result, the shape of epithelial cells appeared less columnar and more cuboidal than in controls (figure 1G). Despite these strong defects, the epithelium retained a characteristic polarised distribution of the apical marker villin, a structural component of microvilli and the tight junction marker cingulin/MAP115 (see online supplementary figure S3). Hence, like in the skin where it nucleates type I hemidesmosomes (containing BP180 and BP230),[17 19–21] α6β4 integrin is essential for the assembly of type II hemidesmosomes (that are lacking BP180 and BP230) present in the intestine, but does not contribute to epithelial polarity.

Loss of intestinal hemidesmosomes impacts on gut barrier function

Loss of α6β4 integrin in the skin affects epithelial integrity.[17 19–21] In the mutant intestine, collagen IV and plectin costaining revealed that the epithelial layer tends to detach from its BM and the subjacent lamina propria (figure 1F, G), without affecting the distribution of the hemidesmosomal laminin γ2 chain (figure 1H). From 3 weeks after birth, areas of epithelial detachment were observed throughout the mutant intestine (see figure 1I and online supplementary figure S4), suggesting that the disruption of hemidesmosomes results in epithelium weakening and loss of firm anchorage to the BM. To confirm these observations, we used a modified method of IEC dissociation[22] in which control and mutant epithelium were subjected to ethylenediaminetetraacetic acid (EDTA) treatment and gentle agitation to assess their ability to resist a slight mechanical stress. Epithelial fragility was significantly increased in the mutant intestines compared with controls as early as 2 days postnatal (P2), and became more prominent at P14 (figure 1J). Alterations affecting the intestinal permeability

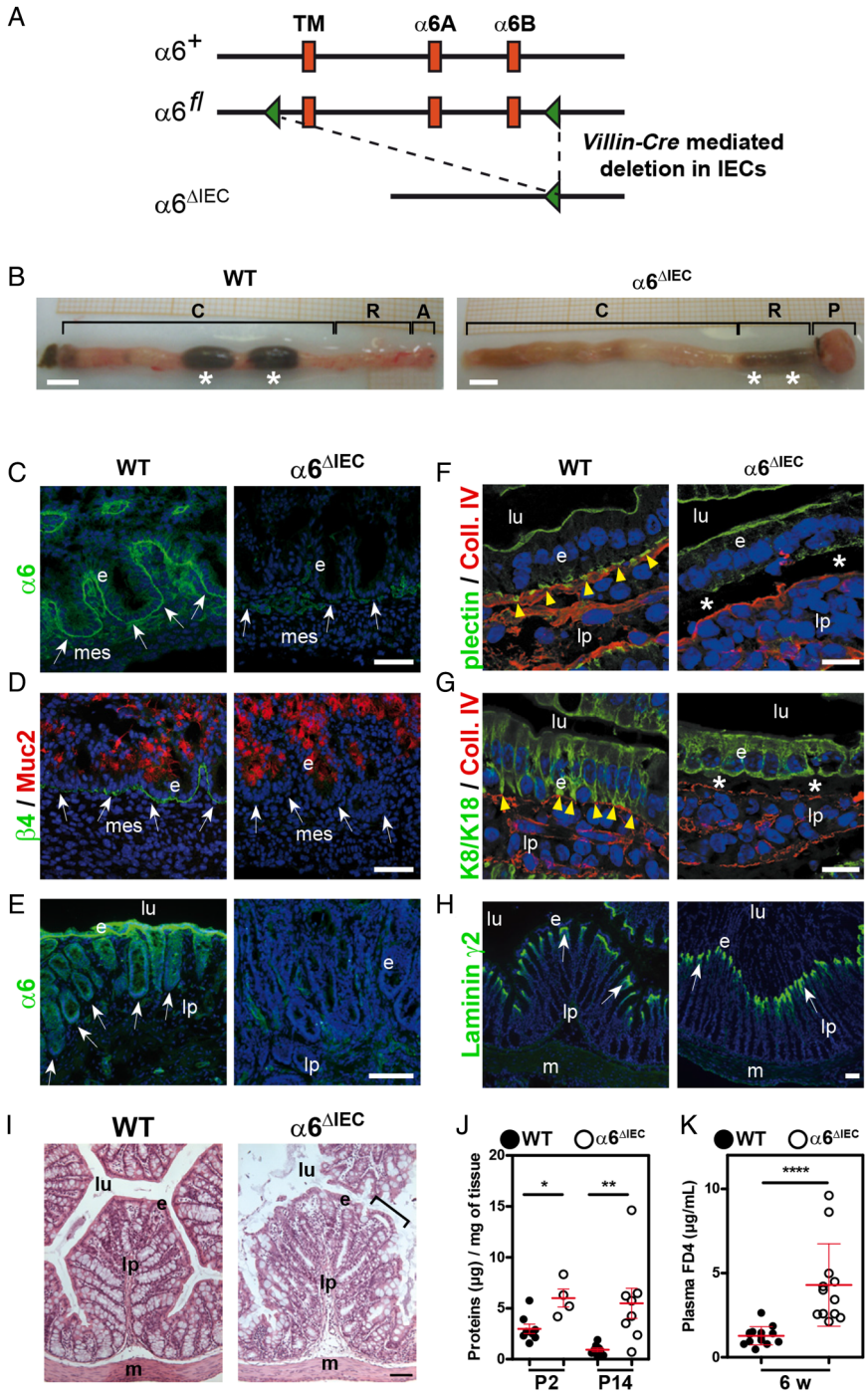

Figure 1 Efficient deletion of *Itga6* in $\alpha6^{\Delta IEC}$ mice results in compromised hemidesmosomes and epithelial fragility. (A) Strategy to generate an intestinal epithelium-specific *Itga6* knockout (for details, see online supplementary figure S1A). The *Itga6* floxed allele ($\alpha6^{fl}$) was obtained after insertion of two *loxP* cassettes (green triangles) at the *Itga6* 3′ end including the TM and the cytoplasmic A and B (α6A; α6B) exons. Crossing of the $\alpha6^{fl/fl}$ mice with the transgenic *Villin-Cre* line results in a truncated *Itga6* copy, denoted $\alpha6^{\Delta IEC}$. (B) Morphology of the colorectal region in 15-week-old WT and $\alpha6^{\Delta IEC}$ mice. White stars indicate stools. Scale bars, 5 mm. (C–H) Immunodetection of hemidesmosome markers in the colon of E16.5 embryos (C and D) and in intestinal segments of mice aged 9–16 weeks (E–H); (E) rectum; (F and G) jejunum; (H) colon; 4′,6-diamidino-2-phenylindole (DAPI) marks nuclei (blue). (C and E) α6-integrin chain and (D) β4-integrin chain (green) with the mucin Muc2 (red). The remaining signal in (C and E) corresponds to α6 integrin in blood vessels, confirming the specificity of the deletion in the epithelium. (F) Plectin and (G) K8/K18 intermediate filaments (green), with collagen IV (red). (H) Laminin-γ2 chain (green). White arrows, epithelium/lamina propria interface; yellow arrowheads, hemidesmosome patches; stars, areas of epithelial detachment in mutants. Scale bars, 50 μm. (I) Histological analysis of the colon from 3-week-old mice; bracket, detached cells from the surface epithelium. Scale bar, 100 μm. (J) Scattered dot plots showing the protein concentration of epithelial cell lysates obtained from small intestinal tissue of pups aged 2 (P2) and 14 (P14) days submitted to a detachment assay; error bars, SD; *p<0.05, **p<0.01. (K) Scattered dot plots showing the plasma concentration of FITC-dextran (FD4) as a measurement of intestinal permeability in 6-week-old animals fed with FD4; error bars, SD; ****$p<10^{-4}$. A, anus; C, colon; e, epithelium; lp, lamina propria; lu, lumen; m, muscle layer; mes, mesenchyme; P, prolapse; R, rectum; TM, transmembrane; w, weeks; WT, wildtype.

are frequently observed in patients with IBD and reflect epithelial barrier dysfunction.[2,3] To examine if such dysfunction occurred in mutant mice, we quantified intestinal permeability in vivo by feeding mice with fluorescein isothiocyanate (FITC)-dextran and measuring FITC levels in the blood plasma. Intestinal permeability was significantly increased in $\alpha6^{\Delta IEC}$ mice (figure 1K). Thus, α6 integrin loss in IECs impairs hemidesmosome formation, epithelial morphology and gut barrier function.

$\alpha6^{\Delta IEC}$ Mice develop spontaneous long-standing extensive colitis

As intestinal barrier defects often lead to inflammation,[1] we examined its potential occurrence in $\alpha6^{\Delta IEC}$ mice. We observed obvious inflammation in all mutants from 6 to 8 weeks of age as clinically illustrated by loose and/or bloody stools, rectal prolapse and mucus discharge when compared with their control littermates (see figures 1B and 2A). The intestinal wall appeared thickened throughout the colorectal region (figure 2B), with a

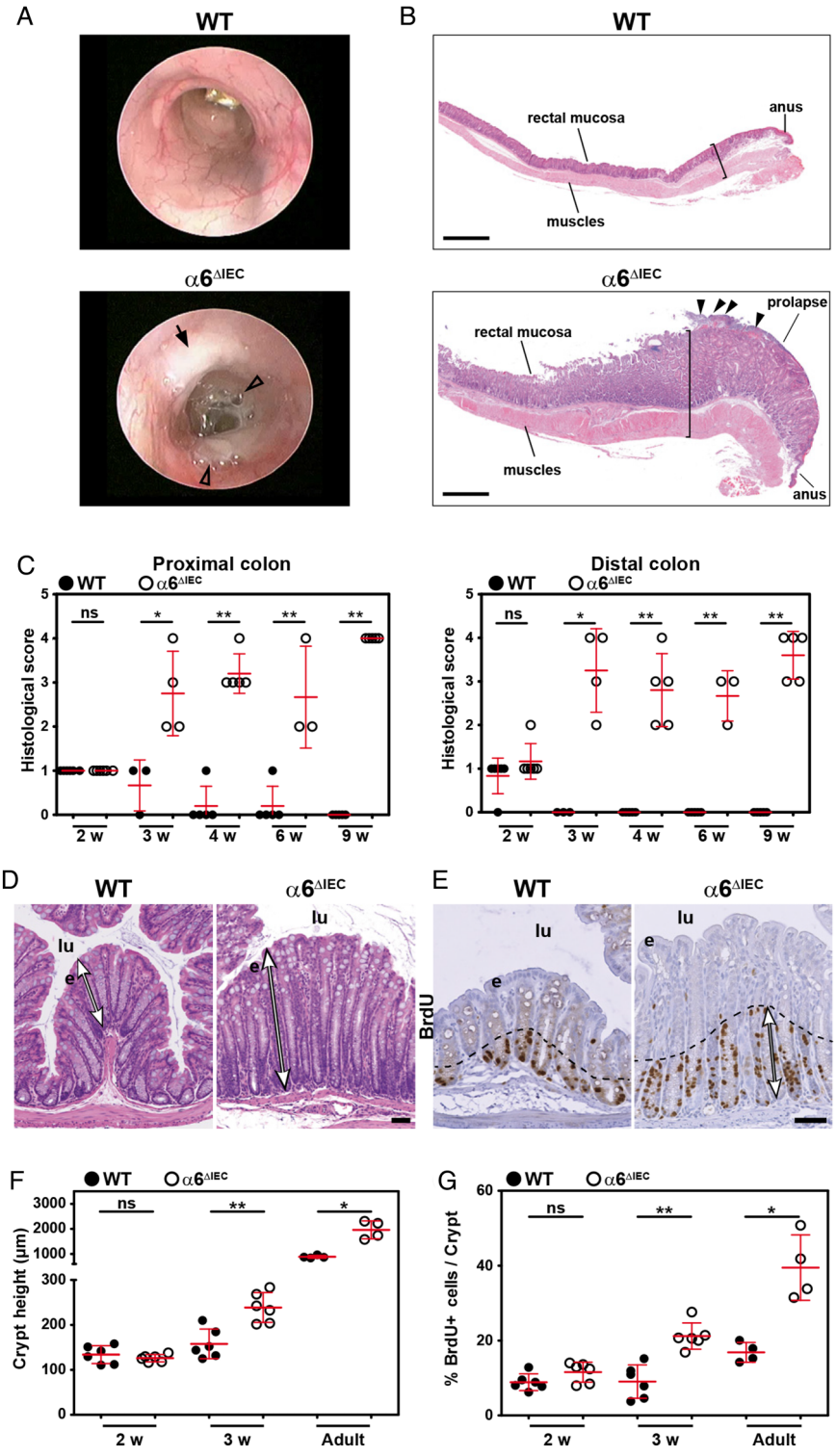

Figure 2 $\alpha6^{\Delta IEC}$ Mice develop colitis soon after weaning. (A) Representative images of WT and $\alpha6^{\Delta IEC}$ adult colons observed by mini-endoscopy. Black arrow, lesion affecting the mutant mucosa; arrowheads, presence of abundant mucinous material in the lumen of the mutant colon. (B) Longitudinal H&E stained sections of the recto-anal region from animals aged 15 weeks. The bracket in mutants highlights the hyperplasia in mucosa and thickened muscle layers (arrowheads, ulcerated surface). Scale bars, 500 μm. (C) Histological scores displayed as scattered dot plots (error bars, SD) measured in the proximal and distal colons of WT and $\alpha6^{\Delta IEC}$ mice from 2 to 9 weeks (w) of age. (D) Transverse H&E stained sections of the distal colons of WT and $\alpha6^{\Delta IEC}$ mice at 4 weeks. Double arrows, crypt height. Scale bar, 50 μm. (E) Immunohistochemical BrdU detection (brown nuclei) on colon sections of 3-week-old animals; dashed lines and double arrows, area of expanded proliferation in the mutant colon. Scale bar, 50 μm. (F and G) Proliferation and crypt height measurement in colons of WT and $\alpha6^{\Delta IEC}$ mice aged 2 and 3 weeks, and adult stages displayed as scattered dot plots (error bars, SD). (F) Quantification of crypt height. (G) Quantification of BrdU-positive cells. *p<0.05, **p<0.01. e, epithelium; lu, lumen; ns, not significant; w, weeks; WT, wildtype.

histological score worsening from 3 weeks after birth (figure 2C). Mutant crypts in the distal colon were on average twice more elongated (figure 2D, F). As early as 3 weeks of age, the proliferation rate was also significantly increased in both colon and rectum of mutants but not in the jejunum as determined by staining for bromodeoxyuridin (BrdU) incorporation (see figure 2E, G and online supplementary figure S5A). These features (figure 2) suggested that $\alpha6^{\Delta IEC}$ mice develop spontaneous long-standing extensive colitis from weaning onwards.

Colitis severity in $\alpha6^{\Delta IEC}$ mice is independent of the adaptive immune response

Studies in mice and humans have strongly suggested that intestinal inflammation results from an impaired innate immune response to the gut microbiota, which results in dysregulation of the adaptive immune system.[7 8] To examine if inflammation in $\alpha6^{\Delta IEC}$ intestine follows this paradigm, we first defined the immunological profile by fluorescence activated cell sorting (FACS) of immune cells isolated from the colonic lamina propria (referred to as lamina propria mononuclear cells).

Mutant mice displayed ~five-fold increase in CD4$^+$ T lymphocytes and of several myeloid cells including neutrophils, dendritic cells and monocytes (figure 3A, B). Notably, there was a >40-fold increased recruitment of Ly-6G$^+$/CD11b$^+$ neutrophils within the colonic mucosa of mutant mice when compared with controls (figure 3B). By contrast, the number of CD8$^+$ T lymphocytes and inflammatory monocytes did not vary (figure 3A, B). Histological analysis confirmed the presence of extensive immune cell infiltrates in the mutant colon/rectum/prolapse area (see online supplementary figure S5B, C). Those were mostly identified as CD11b$^+$ cells by immunostaining, and were recruited as soon as 4 weeks (figure 3C, C′). Of note, the recruitment of these cells was even stronger at 9 weeks (figure 3D, D′).

To formally assess the potential involvement of T lymphocytes and B lymphocytes on disease onset, we crossed $\alpha6^{\Delta IEC}$ mice with *rag1*$^{-/-}$ mice, which lack mature B lymphocytes and T lymphocytes.[24] Remarkably, histopathological analyses revealed that *rag1*$^{-/-}$ $\alpha6^{\Delta IEC}$ double mutant mice developed inflammation similar to that of single *rag1*$^{+/-}$ $\alpha6^{\Delta IEC}$ mutants, with the presence of large immune infiltrates throughout the colorectal mucosa (see online supplementary figure S5C) and high levels of CD11b$^+$ myeloid cells (figure 3E, E′). Collectively, these results demonstrate that the onset of colitis is independent of T lymphocyte and B lymphocyte activation.

We next examined whether the inflammation observed in $\alpha6^{\Delta IEC}$ mice was associated with the MyD88 pathway, a major player of the innate immune response. Colitis occurred similarly in both *MyD88*$^{-/-}$ $\alpha6^{\Delta IEC}$ and *MyD88*$^{+/-}$ $\alpha6^{\Delta IEC}$ mutant animals suggesting that MyD88 signalling was not primarily required to initiate inflammation in $\alpha6^{\Delta IEC}$ intestine (see online

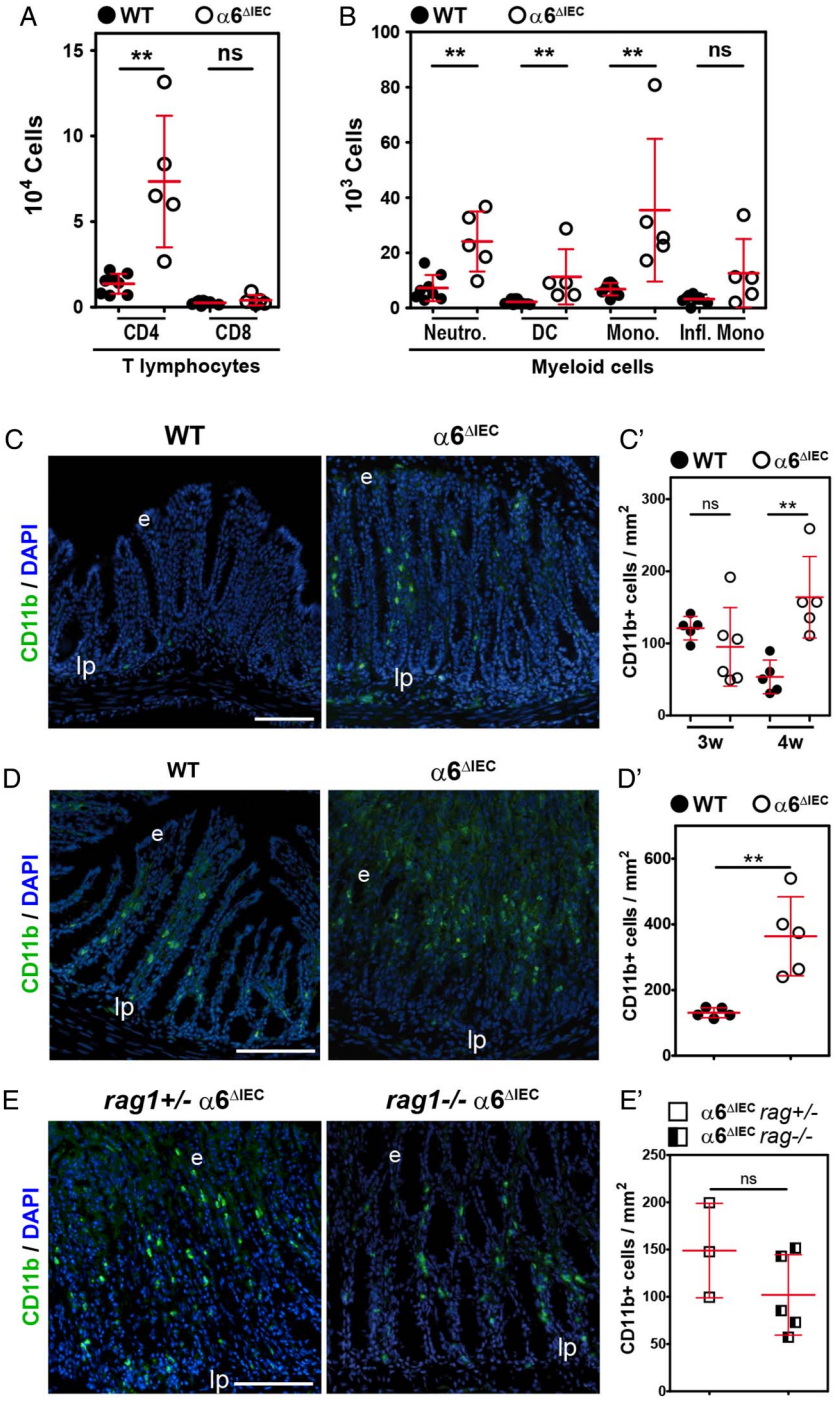

Figure 3 Inflammation onset in $\alpha6^{\Delta IEC}$ mice is mediated by myeloid cells recruitment, independently of the adaptive immune system. (A and B) FACS analysis and quantification of immune cell subpopulations present in colonic lamina propria extracts from animals raised in conventional conditions. LPMCs originate from WT and $\alpha6^{\Delta IEC}$ animals aged 9–15 weeks. Results are displayed as scattered dot plots (error bars, SD); each dot represents the number of positive cells present in the extract for each animal. (A) CD4$^+$ and CD8$^+$ T lymphocytes; (B) Cells of myeloid origin defined as: neutrophils, Ly-6G$^+$ CD11b$^+$; DC, Ly-6G$^-$ CD11c$^+$ MHC class II^{intermediate}; monocytes, Ly-6G$^-$ Ly-6C$^+$ MHC class II$^-$; pro-inflammatory monocytes, Ly-6G$^-$ Ly-6C$^+$ CD11c^{low} MHC class II$^+$ CD64$^+$. (C–E) Immunodetection of CD11b$^+$ cells (green) in the colon of WT and $\alpha6^{\Delta IEC}$ mice aged 4 (C) and 9 (D) weeks, and of combined *rag1*$^{+/-}$ $\alpha6^{\Delta IEC}$ and *rag1*$^{-/-}$ $\alpha6^{\Delta IEC}$ animals (E). Scale bars, 100 μm. (C′–E′) Quantification of the number of CD11b$^+$ infiltrating cells per mm^2 of colon from images illustrated in (C–E), displayed as scattered dot plots (error bars, SD). (C′) WT and $\alpha6^{\Delta IEC}$ mice aged 3 and 4 weeks; (D′) 9-week-old WT and $\alpha6^{\Delta IEC}$ mice; (E′) combined *rag1*$^{+/-}$ $\alpha6^{\Delta IEC}$ and *rag1*$^{-/-}$ $\alpha6^{\Delta IEC}$; *rag1* $\alpha6^{\Delta IEC}$ mice were raised in SPF conditions. **p<0.01. DC, dendritic cells; e, epithelium; FACS, fluorescence activated cell sorting; Infl. Mono, pro-inflammatory monocytes; lp, lamina propria; LPMCs, lamina propria mononuclear cells; MHC, major histocompatibility complex; Mono., monocytes; Neutro., neutrophils; ns, not significant; SPF, specific pathogen-free; w, weeks.

supplementary figure S5D). Hence, inflammation onset did not involve classical toll-like receptor (TLR) pathways going through MyD88.

Early onset of colitis is linked to epithelial caspase-1 activation and IL-18 secretion in α6$^{\Delta IEC}$ mice

To further define the pathways mediating inflammation, we next examined the levels of well-characterised pro-inflammatory cytokines involved in IBD, released by colon explants cultured for 24 hours (see online supplementary materials and methods). Cytokine screening revealed that IL-1β and IL-18 levels were the most prominently increased in mutants compared with controls (see figure 4A and online supplementary figure S6A). Among eight additional cytokines that we assayed, IFNγ, IL-17 and IL-22 levels were also increased in α6$^{\Delta IEC}$ mice, though less prominently (see online supplementary figure S6A, B).

To better characterise the sequence of events occurring during disease onset, we specifically focused on the timing of IL-1β and IL-18 increase relative to the earliest abnormalities observed in mutant mice (see figure 2C–G). In particular, we examined animals aged 2–3 weeks when the epithelial barrier, the immune system and the microbiota are progressively established.[25] We observed a clear difference between the initial secretion of both cytokines, since IL-18 was already significantly increased in the mutant colons at 2 weeks, whereas IL-1β was not detectable at this time point (figure 4B). From 3 weeks onwards, the secretion of both cytokines was significantly increased in the α6$^{\Delta IEC}$ colons (figure 4B).

To identify the most likely cellular source of IL-18 and IL-1β, we used western blot analysis, to screen their expression in whole protein extracts (total colon lysates) and in an enriched epithelial fraction (enriched IECs) obtained by scraping of the colorectal mucosa (see figure 4C and online supplementary figure S7). Since both cytokines are produced as inactive forms (pro-IL-18 and pro-IL-1β) that must be cleaved by caspase-1 to be active and secreted, we also checked the expression of active caspase-1 (resulting from pro-caspase-1 cleavage). Expression levels of pro-IL-18, pro-IL-1β and pro-caspase-1 inactive forms were similar in wildtype (WT) and α6$^{\Delta IEC}$ extracts, regardless of the stage (2 or 3 weeks) or the source of the extract (total colon vs enriched IECs) (see figure 4C and online supplementary figure S7). By contrast, a strong increase of cleaved IL-18 and cleaved caspase-1 was observed in α6$^{\Delta IEC}$ enriched IECs as early as 2 weeks (figure 4C) and was maintained at 3 weeks (see online supplementary figure S7), but was barely detectable in total mutant colon lysates. Cleaved-IL-1β was not or barely detected.

Altogether, our data establish that IL-18 is specifically activated in α6 deficient IECs prior to any clinical and histological signs of colitis, and that its epithelial release precedes the secretion of IL-1β. Furthermore, since the active form of IL-1β was not detected in the mutant IECs, it suggests that it was probably produced by immune cells infiltrating the mucosa.

α6$^{\Delta IEC}$ Colons display defective mucus barrier

One of the factors exacerbating inflammation in patients with IBD comes from defects in the mucus layer that protects from microbial translocation.[3 26] Interestingly, very recent data have linked epithelial IL-18 signalling to mucus production by goblet cells (GCs) and to GC maturation.[27]

To examine the properties of the mucus layer in α6$^{\Delta IEC}$ mice, we used periodic acid Schiff/alcian blue (PAS/AB) staining. We found that the PAS^{+} GC which faced the lumen displayed a larger apical compartment or theca in 4-week-old mutant distal colon (see online supplementary figure S8A–D), as also observed in keratin K8-deficient mice.[28] In addition, the number of PAS^{+} GC detected at the base of the mutant crypts was significantly increased, while the average number of PAS^{+} GC over crypt height was unchanged (see online supplementary figure S8A–D). From 6 weeks of age, Muc2 and PAS/AB staining revealed abundant mucus discharge presenting altered properties in the mutant colonic lumen (see online supplementary figure S8E, F), although the ratio GC/total epithelial cells was similar (59.0 ±4.6% for controls and 59.7±2.7% for α6$^{\Delta IEC}$ mice, n=3). At later stages, the normally bacteria-free inner mucus layer appeared irregular in α6$^{\Delta IEC}$ mice (see online supplementary

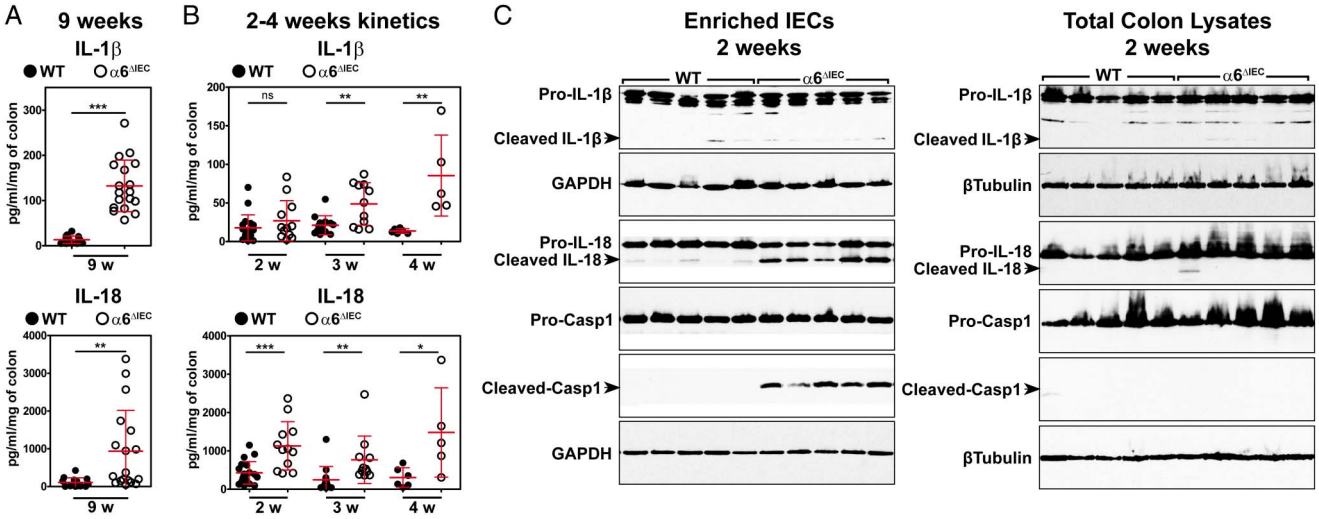

Figure 4 Colitis initiation in α6$^{\Delta IEC}$ mice is triggered by strong epithelial IL-18 secretion and colitis worsening by IL-1β hypersecretion. (A and B) Scattered dot plot quantification of IL-1β and IL-18 levels measured by ELISA starting from colon explants of WT and α6$^{\Delta IEC}$ mice at 9 weeks (A) and at 2, 3 or 4 weeks of age (B) (error bars, SD; ns, not significant; *p<0.05, **p<0.01, ***p<0.001). (C) Western blot analysis performed on protein extracts obtained from an enriched epithelial fraction (enriched IECs) or from whole colon segments (total colon lysates) of 2-week-old WT and α6$^{\Delta IEC}$ mice. Representative blots of three independent experiments performed on at least five animals per group are illustrated. Western blot with GAPDH and β-Tubulin are presented as loading controls. Casp1, caspase-1; enriched IECs, enriched intestinal epithelial cells; GAPDH, glyceraldehyde 3-phosphate dehydrogenase; w, weeks.

figure S8G). To elucidate the potential cause of the mucus defects, we analysed the distribution of the anion transporter SLC26A3 and the Na^+/H^+ exchanger NHE3, described as being involved in the formation and maintenance of the mucus layer,[29–31] and known to be affected in the $K8^{-/-}$ mutant mice.[28] We found that SLC26A3 and to a lesser extent NHE3 were less abundant at the apical surface of $\alpha6^{\Delta IEC}$ colons (see online supplementary figure S8H, H′), arguing for their involvement in the observed mucus defects in association with the altered keratin distribution.

Antibiotic treatment improves disease severity

Alterations of the mucus layer can favour a physical interaction of bacteria with the epithelium.[29 30 32] We thus examined the spatial segregation of the microbiota from the epithelium in the distal colon, using fluorescence in situ hybridisation (FISH) to detect bacterial 16S ribosomal RNA, and Muc2-immunostaining to delineate the mucin layer and the epithelial border. At 3 weeks of age, when histological defects and cytokine levels were already abnormal, bacteria were clearly physically separated from IECs (see online supplementary figure S9A). By contrast, bacteria were attached to the mutant colonic epithelial surface in older diseased mice as judged by the presence of bacterial 16S rRNA in direct contact with IECs (see online supplementary figure S9B).

Given the close contacts between bacteria and mutant IECs, we next assessed whether bacteria had a role in eliciting colitis in $\alpha6^{\Delta IEC}$ mice. We treated 9-week-old animals with a cocktail of broad-spectrum antibiotics prior to collecting intestinal explants in order to deplete a large range of bacterial species. Overall, antibiotics reduced the levels of IL-1β to those observed in untreated controls and halved those observed for IL-18 (see figure 5A and online supplementary figure S9C), and had no effects on the levels of IFNγ, IL-17 and IL-22 (see online supplementary figure S9C). In addition, antibiotics improved disease severity by reducing the number of $CD11b^+$ cells infiltrated into the mutant colonic mucosa (figure 5B), whereas they had no major effect on $CD4^+$ T cells (figure 5B). Consequently, antibiotics reduced the colitis histological score in the mutant colon (figure 5C).

Overall, our results show that bacteria play a role in worsening colitis in $\alpha6^{\Delta IEC}$ mice, but disease onset precedes bacterial attachment to the intestinal epithelial layer. In addition, the fact that antibiotic treatment only partially restored a normal healthy mucosa with normal IL-18 levels further supports the notion that IL-18 plays a key role in triggering inflammation.

α6 Integrin loss in adults recapitulates colitis occurrence observed in $\alpha6^{\Delta IEC}$ animals

To discriminate between direct and indirect effects of α6 integrin ablation, we controlled the timing of *Itga6* ablation in IECs by using the TAM-inducible Cre-ER^{T2} system ($\alpha6^{\Delta IEC\text{-}TAM}$ line).[18] We treated adult mice with TAM at 8 weeks—stage at which animals have a fully mature intestine and immune system—and analysed them 2 weeks later (figure 6A).

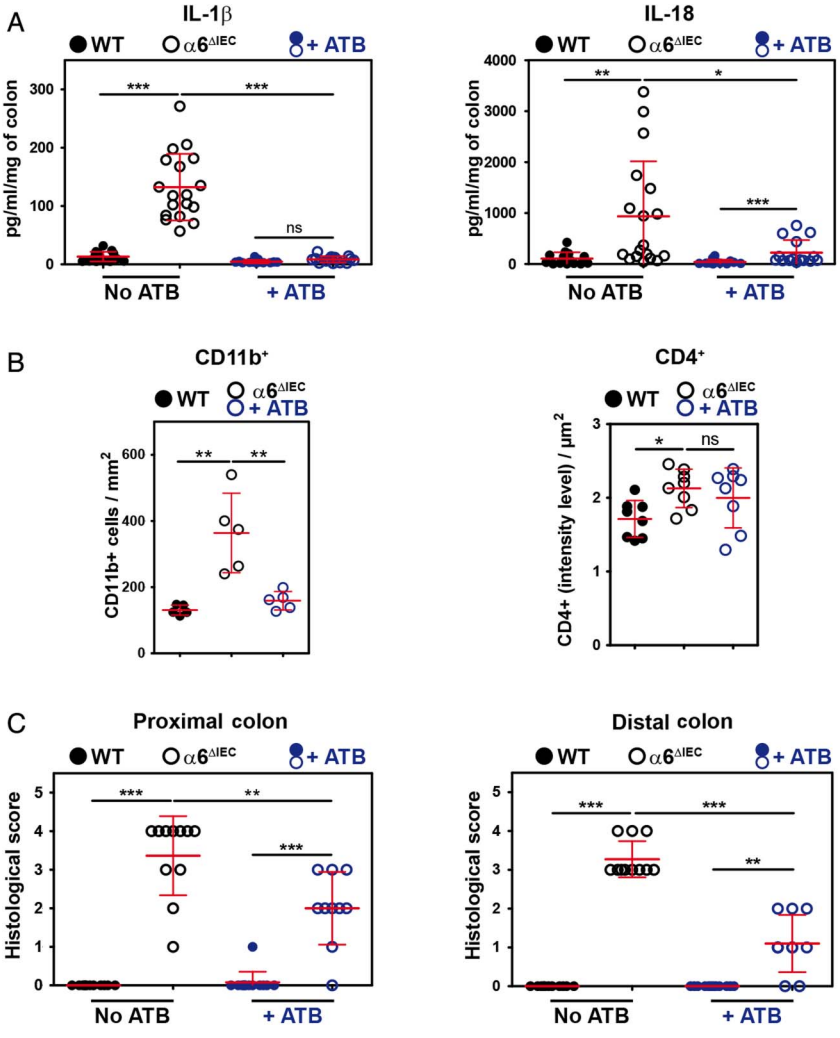

Figure 5 Colitis in $\alpha6^{\Delta IEC}$ mice is partially improved by antibiotic treatment. (A–C) Scattered dot plot representations showing the quantification of cytokine levels measured by ELISA starting from colon explants (A), of the $CD11b^+$ and $CD4^+$ cells infiltrating the colonic mucosa (B), and of histological scores (C), in 9-week-old WT and $\alpha6^{\Delta IEC}$ mice treated with antibiotics (+ATB) or not. In each scattered dot plot, error bars represent SD; *p<0.05, **p<0.01, ***p<0.001. (A) ELISA quantification of IL-1β and IL-18 levels. (B) Quantification of $CD11b^+$ and $CD4^+$ infiltrating cells per surface of colon. (C) Colitis histological scores established in the proximal and distal colons. +ATB, with antibiotics; ns, not significant.

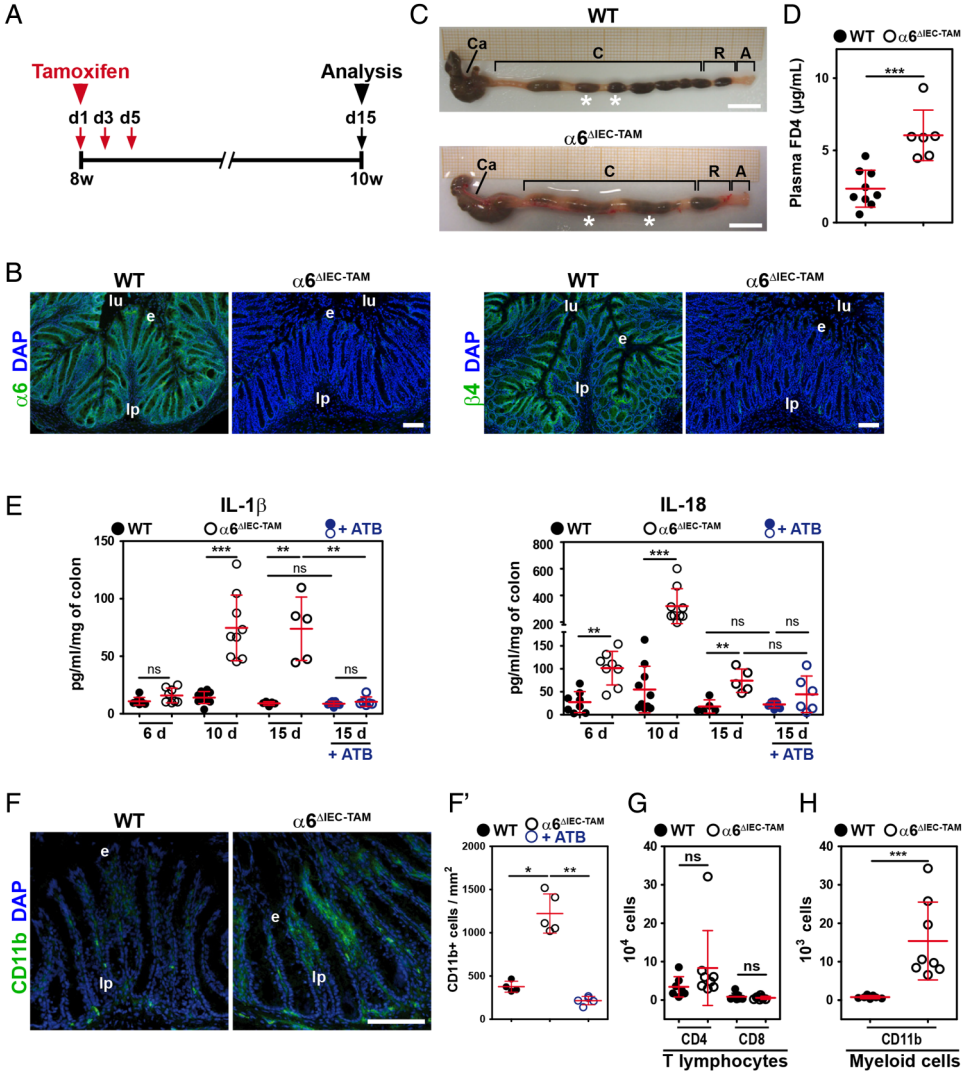

Figure 6 Colorectal inflammation occurs quickly after α6 integrin ablation in adult IECs. (A) Experimental procedure of TAM treatment (red arrows indicate the days of TAM administration) and subsequent analysis (black arrow) of WT and $\alpha6^{\Delta IEC\text{-}TAM}$ mice, illustrated for the time point 15 days post-TAM administration. Animal age is indicated in weeks. (A–D and F–H) Eight-week-old WT and $\alpha6^{\Delta IEC\text{-}TAM}$ mice were treated with TAM and analysed 15 days after the first TAM gavage. (B) Immunodetection of α6-integrin and β4-integrin chains (green) on colon sections of WT and $\alpha6^{\Delta IEC\text{-}TAM}$. DAPI marks nuclei (blue). Scale bars, 50 µm. (C) Morphology of the colorectal region of WT and $\alpha6^{\Delta IEC\text{-}TAM}$ mice. Scale bars, 5 mm. (D) Scattered dot plots showing the plasma concentration of FITC-dextran (FD4) in WT and $\alpha6^{\Delta IEC\text{-}TAM}$ mice fed with FD4; error bars, SD. (E) ELISA quantification of the levels of IL-1β and IL-18 secreted by colon explants cultured for 24 hours. Samples were analysed 6, 10 and 15 days after the first TAM gavage in WT and $\alpha6^{\Delta IEC\text{-}TAM}$ mice treated with antibiotics or not. Results are displayed as scattered dot plots; error bars, SD; ns, not significant. (F and F′) Immunodetection (F) and quantification (F′) of $CD11b^+$ cells (green) in the colon of 10-week-old TAM treated WT and $\alpha6^{\Delta IEC\text{-}TAM}$ mice, 15 days post TAM gavage. Scale bar, 100 µm. (G and H) Quantification by FACS analysis of the immune cell subpopulations present in LPMCs of 10-week-old TAM treated WT and $\alpha6^{\Delta IEC\text{-}TAM}$ mice, 15 days post TAM gavage. (G) $CD4^+$ and $CD8^+$ T lymphocytes; (H) Cells of myeloid origin defined as Ly-$6G^+$ $CD11b^+$. Results are displayed as scattered dot plots (error bars, SD); each dot represents the number of positive cells present in the extract for each animal. *p<0.05; **p<0.01; ***p<0.001. A, anus; Asterisks (*), stools; +ATB, with antibiotics; C, colon; Ca, caecum; d, day; e, epithelium; FACS, fluorescence activated cell sorting; IECs, intestinal epithelial cells; LPMCs, lamina propria mononuclear cells; lp, lamina propria; lu, lumen; ns, not significant; R, rectum; TAM, tamoxifen; w, week.

Immunodetection of α6β4 integrin in $\alpha6^{\Delta IEC\text{-}TAM}$ colons revealed an efficient and homogeneous removal of the α6 and β4 signals in the mutant IECs (figure 6B). Interestingly, $\alpha6^{\Delta IEC\text{-}TAM}$ mutants displayed colorectal swelling and loose stools (figure 6C), and an increased intestinal permeability (figure 6D) similar to those observed in the $\alpha6^{\Delta IEC}$ line. To better define how early molecular signs of colitis arise, we examined animals at 6, 10 and 15 days post-TAM administration. At day 6 post-TAM, mutant colons displayed significant epithelial detachment and an increase in IL-18 secretion (see figure 6E and online supplementary figure S10A, B), as what also observed in $\alpha6^{\Delta IEC}$ animals (see figures 1I, 4B and online supplementary figure S4B, C). $\alpha6^{\Delta IEC\text{-}TAM}$ Mutant mice started to develop hyperplasia (assessed by the proliferative marker Ki-67), $CD11b^+$ cell infiltration and increased IL-1β secretion at days 10 and 15 post-TAM (see figure 6E–F′ and online supplementary figure S10A–D), with no difference in T lymphocyte subsets (figure 6G, H). In line with our previous findings in the constitutive $\alpha6^{\Delta IEC}$ model, antibiotic treatment applied prior to TAM administration reduced signs of inflammation (see figure 6E–F′ and online supplementary figure S10), without reducing epithelial detachment and restoring IL-18 secretion to

control levels (see figure 6E and online supplementary figure S10). Thus, $\alpha6^{\Delta IEC\text{-}TAM}$ mice phenocopied the $\alpha6^{\Delta IEC}$ line.

We next aimed at further delineating the molecular signature of inflammation upon loss of the α6β4 integrin. To this end, we performed a transcriptome analysis on mRNAs extracted from the rectal compartment of WT and $\alpha6^{\Delta IEC\text{-}TAM}$ mice 15 days post-TAM treatment. Microarray data (Affymetrix) were analysed using the 'Ingenuity Pathway Analysis' (IPA) which helped us to define molecular interaction networks. The most activated network in $\alpha6^{\Delta IEC\text{-}TAM}$ mutants included the gene encoding IL-1β (see online supplementary figure S11A), confirming the leading role of the latter regulatory circuit in disease severity. Additional genes with ascribed function related to this 'IL-1β-inflammatory network' encoded pro-inflammatory molecules (IL1-RL1, CXCL5/CXCL6 and CXCR2) or extracellular matrix (ECM) remodelling factors (such as MMP10). Their differential expression was validated by RT-qPCR (see online supplementary figure S11B).

Altogether the phenocopy of colitis in adults having an already well-established immune system and microbiota highlights that the origin of colitis in the absence of α6 integrin is primarily associated with IEC detachment from the BM, secretion of epithelial IL-18 and exacerbation due to bacteria.

The spontaneous and fully penetrant development of adenocarcinomas in $\alpha6^{\Delta IEC}$ mice requires activation of B lymphocytes and T lymphocytes

Some animal models of IBD can develop adenocarcinomas, although at a low prevalence unless treated with dextran sodium sulfate and azoxymethane.[7 33] By contrast, we observed that all $\alpha6^{\Delta IEC}$ mice spontaneously developed colorectal adenocarcinomas by 1 year of age, and without any further chemical treatment. Adenocarcinomas and/or high-grade dysplasia were mostly located in the rectal prolapse (figure 7A), and were found very rarely in the small intestine (two out of the eight cases analysed). Histopathological analyses revealed different degrees of mucosal infiltration (figure 7B) and numerous Ki-67 positive cells were observed in invading glands within the rectal prolapse (figure 7C). Among 14 mutant mice aged 48–80 weeks, all had adenocarcinomas (figure 7D). Interestingly, $\alpha6^{\Delta IEC\text{-}TAM}$ mice treated with TAM at 8 weeks and analysed 1 year later or more developed also adenocarcinomas / high grade dysplasia (five out of the seven cases analysed) or at least low grade dysplasia (2/7) in the rectal prolapse, indicating that the depletion of α6 integrin even when induced in the mature intestine can trigger colitis-associated carcinogenesis (figure 7D). We next used positron emission tomography (PET scan) to test for the presence of metastasis. We detected a high metabolic level of fluorodeoxyglucose (FDG) uptake in the whole large intestine of 1-year-old $\alpha6^{\Delta IEC}$ mice, but failed to observe distant metastasis (figure 7E).

As reported above, the adaptive immune system does not play an obvious role in the onset of colitis. To define whether or not activation of the adaptive immune system might also be dispensable for progression to adenocarcinomas, we compared single $\alpha6^{\Delta IEC}$ and $rag1^{-/-}$ $\alpha6^{\Delta IEC}$ double mutant mice raised in specific pathogen-free (SPF) conditions. Out of eight $\alpha6^{\Delta IEC}$ animals aged 45–76 weeks, three had developed an adenocarcinoma, one displayed a severe dysplasia, whereas the four remaining had inflammation (figure 7D). By contrast, none of the 50–64 weeks old $rag1^{-/-}$ $\alpha6^{\Delta IEC}$ double mutants (6/6) developed an adenocarcinoma; instead they showed very discrete low grade dysplasia lesions (4/6) and chronic inflammation (6/6) (figure 7D, F), suggesting a critical role for the T and B cell activation on disease progression.

To know if local alterations of the microenvironment, in particular of the laminins, might contribute to tumour development, WT and mutant rectal tissues were immunostained with laminin γ2, the hemidesmosome ligand of α6β4, that is known to be overexpressed and associated with poor prognosis in CRC.[34] Large laminin γ2 deposits were detected throughout the whole tumoural area within the rectal prolapse in mutant mice while the signal was restricted to the BM at the upper part of the crypts in controls (figure 7G).

Finally, to better understand the mechanisms underlying tumour aggressiveness, we defined the specific transcriptomic signature associated with carcinogenesis in the $\alpha6^{\Delta IEC}$ model by comparing gene expression in three distinct samples: (1) adenocarcinoma-comprising areas from the mutant prolapse, (2) inflamed but non-cancerous adjacent rectal mucosa and (3) rectal mucosa obtained from WT mice. A first IPA analysis allowed to identify significantly overexpressed or underexpressed genes in the tumour areas versus the inflamed mucosa (Student's t-test, p value ≤ 0.001; fold change $\geq +2$ or ≤ -2) and to define the most activated gene network in the tumours (see online supplementary figure S12A). Many molecules involved in ECM composition and degradation/remodelling, as well as inflammatory components belong to this genes network. Interestingly, several of them have been described as being involved in colorectal carcinogenesis such as MMP9, MMP13 or TIMP1 (for review see ref. [35]) or in inflammatory pathways (for review see ref. [36]). Moreover, as previously described for the inflammation worsening, network analysis emphasised the prominent role of IL-1 cytokines and IL-1R signalling, suggesting that this inflammatory signature was required for tumour progression.

We further characterised the molecular signature of inflamed or cancerous lesions comparing them to the normal rectal mucosa by using a second IPA analysis which revealed the different categories of gene functions significantly affected. The results are summarised in online supplementary table S1 and figure S12B.

Altogether, the intestinal inflammation observed in $\alpha6^{\Delta IEC}$ mice results from epithelial detachment and IL-18 secretion leading to defective mucus barrier, independently of T lymphocyte and B lymphocyte activation and of MyD88 signalling. Furthermore, our results suggest that intestinal tumourigenesis is likely caused by continuous IL-1 signalling together with BM remodelling and B cell and T cell activation.

DISCUSSION

We report for the first time the key physiological protective function of the α6 integrin-mediated signalling in IECs against intestinal inflammation and tumourigenesis in mice. Our data suggest that the sequence of events leading to inflammation after intestinal epithelial-specific *Itga6* ablation during development or induced in adults, first entailed hemidesmosome disruption leading to IEC detachment from the BM and to epithelium weakening. In turn, this induced sustained caspase-1 activation and IL-18 secretion in damaged IECs. Subsequently, the mucus barrier became progressively defective, promoting the exposure of IECs to bacterial and/or luminal components. Consequently, chronic inflammation was mediated by IL-1β oversecretion and myeloid cell accumulation. Importantly, the same cascade of events was observed when *Itga6* deletion was induced in the adult intestine, ruling out indirect cumulative effects related to developmental defects. Finally, all $\alpha6^{\Delta IEC}$ and $\alpha6^{\Delta IEC\text{-}TAM}$

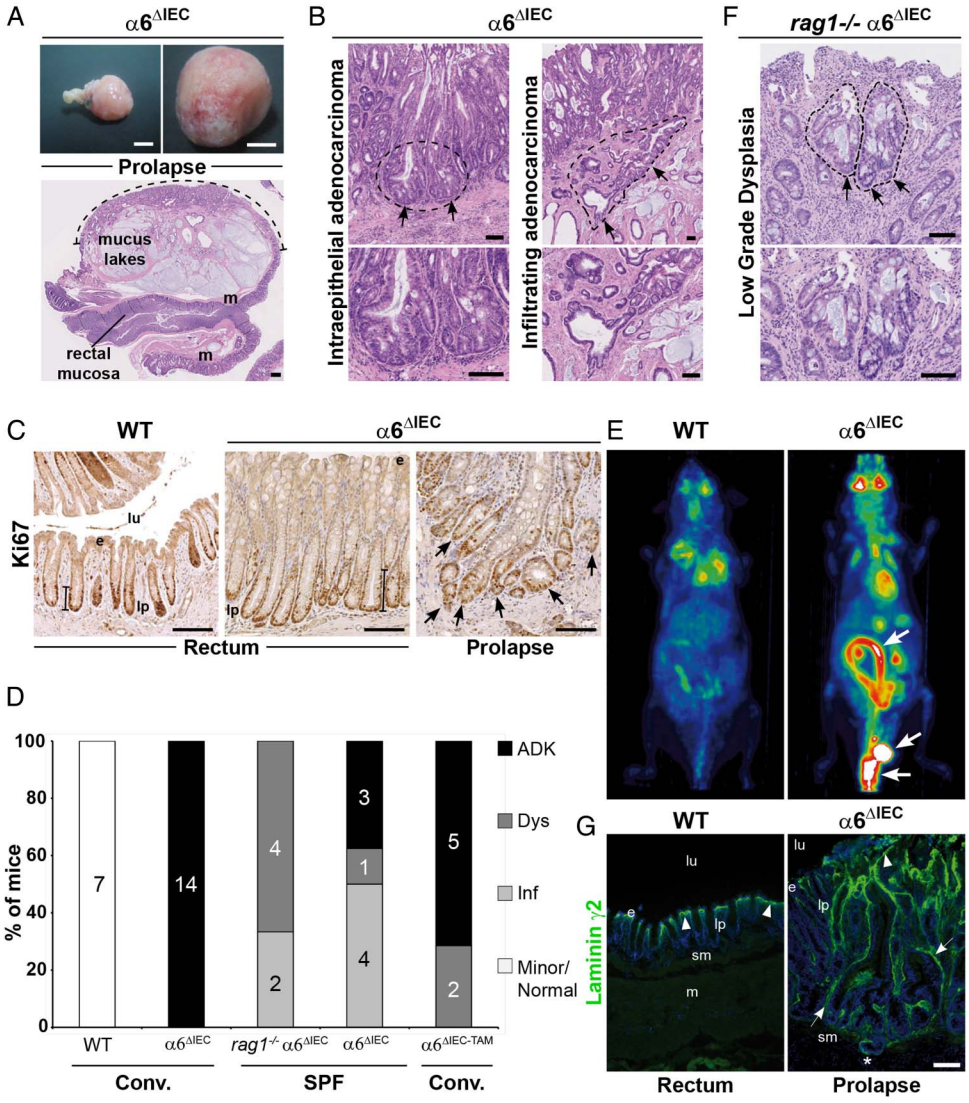

Figure 7 All $\alpha6^{\Delta IEC}$ mice spontaneously develop colitis-associated adenocarcinomas. (A–G) Tumour features in ≥1-year-old $\alpha6^{\Delta IEC}$ mutant mice. (A) Wide-field view (top) and histological section (bottom) of a large prolapse with an infiltrating mucinous adenocarcinoma invading the submucosa and muscle layers (m). Dotted line, region comprising tumour lesions. Scale bars: 5 mm (top); 500 μm (bottom). (B) Views of prolapse-associated tumours: (left) intraepithelial adenocarcinoma and (right) highly infiltrating adenocarcinoma (dotted lines, arrows). Higher magnifications are shown in the lower panels. Scale bars: 100 μm. (C) Ki67 immunostaining (brown nuclei) on rectal sections from 1-year-old WT and $\alpha6^{\Delta IEC}$ mice. Ki67^{+} cells are located at the base of the crypts (bar), and in the invading glands of the prolapse associated-adenocarcinoma (right panel, arrows). Scale bars: 100 μm. (D) Schematic representation showing the repartition of 1-year-old affected mice according to their genotype and the type of intestinal lesions they displayed; numbers mentioned in histogram columns and percentage (*y*-axis) of affected mice as well as the lesion types are indicated. The genotype of mice and the housing conditions (conventional (conv.) vs SPF) are indicated under the chart. (E) FDG-PET images of WT and $\alpha6^{\Delta IEC}$ mice showing a significant FDG uptake in the mutant large intestine and the rectal prolapse area (arrows). (F) Section through the recto-anal region of a combined *rag1*$^{-/-}$ $\alpha6^{\Delta IEC}$ mutant showing a low grade dysplasia (dotted line, arrows). Lower panel: high magnification of the dysplasia. Scale bars: 100 μm. (G) Immunodetection of laminin γ2 chain (green) in WT rectum and $\alpha6^{\Delta IEC}$ prolapse. DAPI (in blue) marks nuclei. Arrowheads, basement membrane underlying the surface epithelium. Arrows, increased deposits of laminin γ2 in the basement membrane and around tumour areas in $\alpha6^{\Delta IEC}$ prolapse. Asterisks (*), invasive gland infiltrated into the sm. Scale bar: 100 μm. ADK, adenocarcinoma; Dys, low grade dysplasia; e, epithelium; FDG, fluorodeoxyglucose; Inf, inflammation; lp, lamina propria; lu, lumen; m, muscle layer; sm, submucosa; SPF, specific pathogen-free; PET, positron emission tomography.

animals developed spontaneous infiltrating tumours after 1 year without any further chemical treatment. Such tumour development was dependent on the activation of the adaptive immune system (figure 8).

We suggest that defective α6 integrin function at the hemidesmosome, and its induced mechanical epithelial fragility, is ultimately responsible for colitis. The concomitant loss of the β4 integrin subunit, which has already been observed in *Itga6* knockout,[17 20 37] might unbalance some signalling events modulated by this integrin chain,[38] and could thereby trigger caspase-1 activation and IL-18 secretion. Expression of the β1 integrin chain was not significantly affected in $\alpha6^{\Delta IEC}$ mice, consistent with the fact that β1 depletion in the intestine led to more severe phenotypes.[39] We further suggest that the absence of stable hemidesmosomal junctions leads to a reduced capacity of IECs to resist mechanical stress, leading to epithelial detachment in particular at weaning when such stress dramatically increases due to changes in diet and amplification of muscle

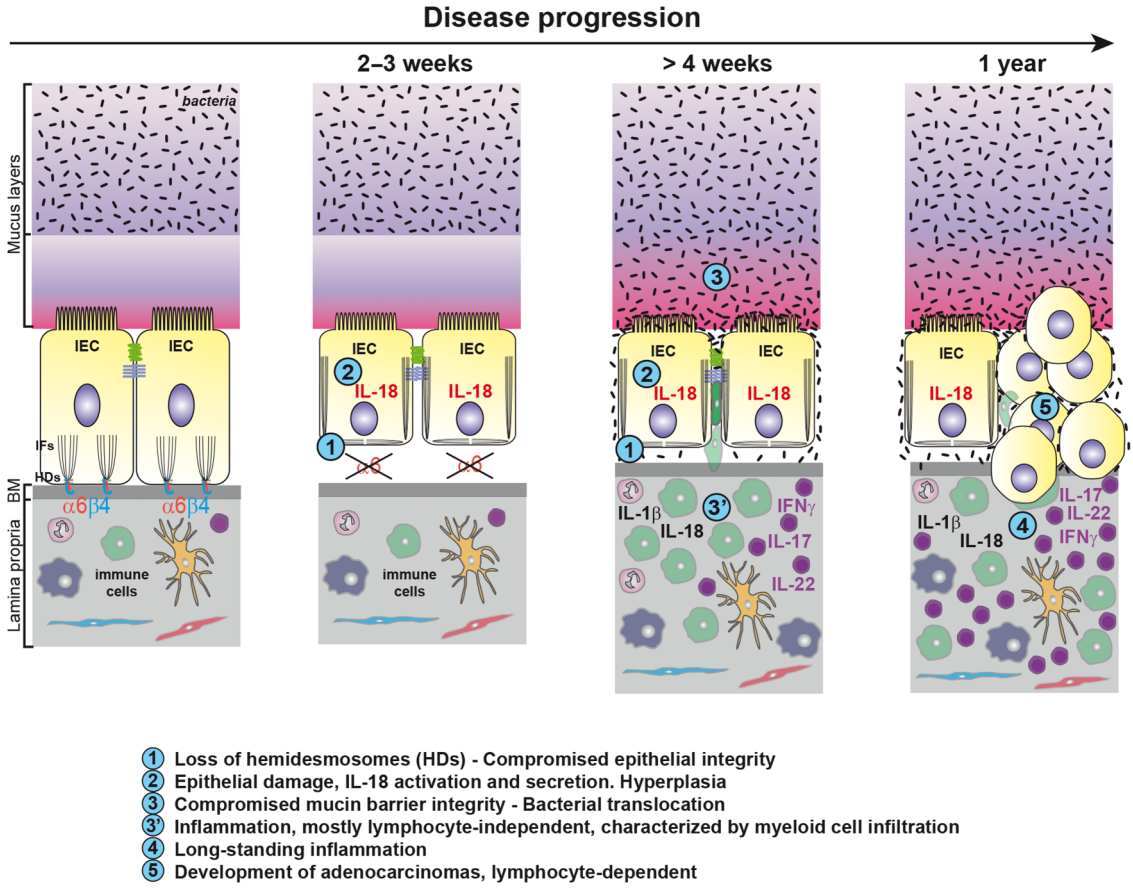

Figure 8 Model of the sequence of events leading to colorectal inflammation and carcinogenesis. Schematic drawing illustrating two IECs of the large intestine attached through α6β4 integrin to the BM via the HDs. By compelling the data obtained from $\alpha6^{\Delta IEC}$ and $\alpha6^{\Delta IEC\text{-}TAM}$ models, we suggest that the following sequence of events occurs. First, loss of the integrin impairs epithelial integrity causing epithelium fragility and detachment from the BM. The absence of tight anchorage to the BM results in disruption of the IFs network and impaired cell architecture. Second, epithelial damage triggers activation of caspase-1 in IECs followed by a drastic activation and secretion of IL-18. Intestinal permeability increases, and hyperplasia occurs in the epithelium (not illustrated). Third, presumably as a secondary consequence (defective cytoskeleton, changes in mucosal pH, cytokine release), the integrity and composition of the mucin layer become altered, favouring bacterial penetration and translocation. Concomitantly, altered epithelial barrier function triggers an inflammatory response, induced in part by exposure of the immune system to bacteria. Inflammation relies on engagement of the innate immune system, mostly independently of the lymphocyte-mediated immunity. It is characterised by enhanced secretion of epithelial IL-18 and immune-mediated IL-1β, and infiltration of $CD11b^+$ myeloid cells into the colonic mucosa. In parallel, lymphoid cells secrete IL-17, IL-22 and IFNγ and sustain chronic inflammation over a long period. Lastly, perpetuation of long-standing colitis associated with alterations of the microbiota invariably induces the spontaneous development of adenocarcinomas in all $\alpha6^{\Delta IEC}$ mutants, tumour progression being dependent on the adaptive immune system. BM, basement membrane; HDs, hemidesmosomes; IECs, intestinal epithelial cells; IFs, intermediate filaments.

contractions. The role of mechanical stress in the induction of a severe intestinal dysfunction has been shown in mice deficient for the integrin-associated protein kindlin-1, in which IECs fail to properly adhere to the BM and to form an efficient epithelial barrier, resulting in a severe colitis and perinatal lethality.[40] Intestinal dysfunction due to α6β4 integrin absence in the intestine and a complete epithelium detachment, was also reported in a clinical case, and supports our findings.[41] Interestingly, it has also been shown that hemidesmosome disturbance in *Caenorhabditis elegans* epidermis triggers an innate immune response.[42]

The activation of IL-18 downstream of the epithelial detachment induced by α6 integrin loss occurs independently of MyD88 through yet unknown mechanisms. As the caspase-1 is activated, we speculate that epithelial detachment leads to mechanical stress damage signals triggering the assembly of an inflammasome, which remains to be identified. Alterations that accumulate as a result of these initial inflammatory signals greatly contribute to increase disease severity. In particular, impairment of the mucus barrier and the subsequent exposure of the epithelial mucosa to bacterial compounds can exacerbate colitis, as was observed in mice displaying defective mucus due to the loss of core 1-derived *O*-glycans.[43] Mucosal defects in $\alpha6^{\Delta IEC}$ mice are presumably caused by: (i) the abnormal localisation of keratins K8/18,[28 44] (ii) the abnormal distribution of the ion transporters SLC26A3 and NHE3, implicated in mucus barrier formation[29–31] and (iii) increased levels of IL-18, which controls the maturation and secretion of the mucus.[27] Interestingly, it has been suggested that IL-18 controls the maturation of GCs by regulating the expression of the transcription factors Gfi1, Spdef and KLF4.[27]

Mechanistically, we identified that inflammation worsening required innate but not adaptive immunity mainly through the secretion of IL-1β, presumably by the infiltrating $CD11b^+$ myeloid cells as a consequence of greater bacterial translocation. We also suggest that bacteria strongly contribute to exacerbate disease severity in our models, since antibiotic treatment strongly lowered IL-1β secretion levels, and partially IL-18. Mutant

$\alpha6^{\Delta IEC}$ mice also displayed enhanced and antibiotic-insensitive IL-17, IL-22 and IFNγ levels, which might contribute to inflammation and later to adenocarcinoma formation, since IL-17 and IL-22 have been involved in tumour progression.[45–47]

A most notable feature of the $\alpha6^{\Delta IEC}$ model is the spontaneous development of colorectal adenocarcinomas, which had not been observed to occur with full penetrance in previously described mouse models of intestinal inflammation.[33] Unexpectedly, the IBD-like phenotype observed in mice deficient in keratin-8 (K8), another key component of intestinal hemidesmosomes, relies on T lymphocytes rather than myeloid cells but was not sufficient to lead to carcinoma development.[28 48 49] The latter findings suggest that hemidesmosome function was not similarly affected in $K8^{-/-}$ and $\alpha6^{\Delta IEC}$ models. In K8 deficient colon, the β4 integrin was overexpressed and led to the activation of survival signals mediated by focal adhesion kinase (FAK) phosphorylation, suggesting that the hemidesmosomes remained at least partially functional.[50] By contrast, hemidesmosomes were totally disrupted in the intestine of *Itga6*-deficient mice, which probably led to an altered signalling cascade and keratin network.

Based on the tumourigenesis observed in $\alpha6^{\Delta IEC}$ mice, α6β4 integrin could be classified as a tumour suppressor. This conclusion seems at odds with other results establishing that α6β4 integrin behaves as an oncogene when it cooperates with ErbB2 in the formation of mammary tumours.[51] However, the function of α6β4 is fully dependent on the tissue context.[52] Likewise, in the skin, α6β4 integrin can either suppress or promote tumour growth depending on whether or not cells express Ras (V12), which is the oncogenic form of the small GTPase.[53]

In future studies, it will be important to further assess whether it is the microbiota imbalance, changes in the homeostasis of the immune system or some other factors that play a prevalent role in tumour formation. Besides host-microbiota interactions, mechanical stress might also influence the process, since adenocarcinomas appeared mostly in the rectal region which is the most intensely subjected to such stress and to interactions with the gut microbiota. Interestingly, hemidesmosomes have recently been found to act as a mechanotransduction platform;[54] in this framework, the lack of response to mechanical stimuli in $\alpha6^{\Delta IEC}$ mice might contribute to impair epithelial homeostasis.

A large number of studies, mainly based on the development of genetically engineered mouse models,[33] have been conducted for many years to define the origin of colitis-associated CRC. In this study we revealed the key role of the integrin/BM connection and suggest that besides microbial cues, biomechanical cues contribute to intestinal homeostasis. The key interest of the $\alpha6^{\Delta IEC}$ line is that it recapitulates most of the events occurring during colitis-associated carcinogenesis, with alterations very similar to those observed in many patients with IBD at high risk of developing CRC. In addition, our molecular characterisation of tumours bring new interesting leads for understanding the mechanisms involved in the progression of colitis-associated cancer. Thereby, the $\alpha6^{\Delta IEC}$ model provides valuable tools to develop new preventive/curative treatments for such unpredictable and invalidating diseases.

MATERIALS AND METHODS

The generation of mouse lines, their manipulation and other specific analyses (antibiotic treatment, epithelial cell detachment assay, FITC-dextran assay, endoscopy, histological analysis, immunofluorescence, immunohistochemistry, FISH, FACS analysis, image analysis, cytokine measurements, preparation of colon protein extracts and western blotting, RT-qPCR, transcriptome analysis, FDG-microPET imaging and study approval) as well as statistics used in this study are described in online supplementary materials and methods.

Author affiliations
[1]Department of Development and Stem Cells, Institut de Génétique et de Biologie Moléculaire et Cellulaire (IGBMC), Université de Strasbourg, Illkirch, France
[2]Inserm, U964, Illkirch, France
[3]CNRS, UMR 7104, Illkirch, France
[4]Université de Strasbourg, Strasbourg, France
[5]Current address: F. Widjaja Foundation Inflammatory Bowel & Immunobiology Research Institute, Department of Medicine, Cedars Sinai Medical Center, Los Angeles, California, USA
[6]Inserm, U1109, MNT3 Team, Strasbourg, France
[7]Current address: Department of Functional Genomics and Cancer, IGBMC, Illkirch, France
[8]CNRS, Inserm, CHU Lille, Institut Pasteur de Lille, U1019—UMR 8204—CIIL—Centre d'Infection et d'Immunité de Lille, Université de Lille, Lille, France
[9]Inserm, Université de Lille, CHRU Lille, UMR-S 1172—Jean-Pierre Aubert Research Center, Lille, France
[10]LabEx Medalis, Université de Strasbourg, Strasbourg, France
[11]Fédération de Médecine Translationnelle de Strasbourg (FMTS), Strasbourg, France
[12]CHRU Strasbourg, Hôpital de Hautepierre, Service d'anatomo-pathologie, Strasbourg, France
[13]Current address: Département de Pathologie, Institut Bergonie, Bordeaux, France
[14]UMR1319—MICALIS Institute, INRA, AgroParisTech,Université Paris-Saclay, Jouy-en-Josas, France
[15]CNRS, UMR 7178, Institut Pluridisciplinaire Hubert Curien, Strasbourg, France
[16]Current address: NORLUX Neuro-Oncology Laboratory, CRP-Santé, Luxembourg
[17]Institut Curie, Paris, France
[18]CNRS, UMR 144, Paris, France
[19]Current address: UMR7622, IBPS, Université Pierre et Marie Curie, Paris, France

Acknowledgements We thank D Ferrandon, D Louvard, T Mayadas, J-M Reichhart, B Reina and L Sorokin for critical reading of the manuscript, A Klein and C Arnold for technical assistance, C Ebel for help with FACS analysis, J-P Ghnassia for anatomopathogical analysis, the IGBMC-histology platform for technical support, J Pontabry for CD4-SLC26A3 image analysis, L Cao (Inviscan SAS) for PET scan image reconstruction, M-F Champy for cytokine multiplex measurements, C Thibault-Carpentier and V Alunni for microarray analysis, A Van Es and the IGBMC animal facility staff for help and advice in animal experimentation, D Metzger, P Chambon, M Li, S Chan and T Sasaki for gift of reagents and S Bour for help in figure preparation.

Contributors EG-L conceived and supervised the project until mid-2012; ADA and ML supervised the project afterwards. EG-L and ADA generated the $\alpha6^{\Delta IEC}$ mice. ADA characterised the phenotypes. HH developed and analysed the $\alpha6^{\Delta IEC\text{-}TAM}$ line, and contributed to IPA analysis. FA, OL, PS-A and MK made the initial phenotype description. SN and MC analysed the microbial flora and ELISA assays. SS, VP and S Rodius assisted ADA for various technical aspects. EB and IVS examined some mucus defects. AM-N performed anatomo-pathological analyses. AM-N and MC assessed the histological scores. P Laquerriere performed PET scan analysis. DD contributed in Affymetrix and IPA analysis. P Lepage realised the bacterial bioinformatics analysis. ADC performed ELISA experiments. S Robine provided the Villin-Cre transgenic lines. ML and ADA wrote the manuscript, with inputs from EG-L, PSA and MC.

Funding This work was supported by funds from CNRS, Inserm and Université de Strasbourg, by grants from the Association pour la Recherche sur le Cancer and Ligue Régionale contre le Cancer (EG-L), the Fondation pour la Recherche Médicale ('Equipe FRM 2009' to MC), the Institut National du Cancer (Appel à projets 'Formes précoces du cancer colorectal' to EG-L and PS-A and to EG-L and MC), Agence Nationale pour la Recherche (EG-L and ML) and LabEx INRT (IGBMC, UdS). SN was a recipient of a Postdoctoral Fellowship from the Ligue contre le Cancer.

Competing interests None declared.

Provenance and peer review Not commissioned; externally peer reviewed.

REFERENCES

1 McGuckin MA, Eri R, Simms LA, *et al*. Intestinal barrier dysfunction in inflammatory bowel diseases. *Inflamm Bowel Dis* 2009;15:100–13.
2 Okamoto R, Watanabe M. Role of epithelial cells in the pathogenesis and treatment of inflammatory bowel disease. *J Gastroenterol* 2016;51:11–21.

3 Salim SY, Söderholm JD. Importance of disrupted intestinal barrier in inflammatory bowel diseases. *Inflamm Bowel Dis* 2010;17:362–81.
4 Abraham C, Cho JH. Inflammatory bowel disease. *N Engl J Med* 2009;361:2066–78.
5 Grivennikov SI. Inflammation and colorectal cancer: colitis-associated neoplasia. *Semin Immunopathol* 2013;35:229–44.
6 Ullman TA, Itzkowitz SH. Intestinal inflammation and cancer. *Gastroenterology* 2011;140:1807–16.
7 Kaser A, Zeissig S, Blumberg RS. Inflammatory bowel disease. *Annu Rev Immunol* 2010;28:573–621.
8 Maloy KJ, Powrie F. Intestinal homeostasis and its breakdown in inflammatory bowel disease. *Nature* 2011;474:298–306.
9 Spenlé C, Hussenet T, Lacroute J, *et al*. Dysregulation of laminins in intestinal inflammation. *Pathol Biol* 2012;60:41–7.
10 Nievers MG, Schaapveld RQ, Sonnenberg A. Biology and function of hemidesmosomes. *Matrix Biol* 1999;18:5–17.
11 Stutzmann J, Bellissent-Waydelich A, Fontao L, *et al*. Adhesion complexes implicated in intestinal epithelial cell-matrix interactions. *Microsc Res Tech* 2000;51:179–90.
12 Barrett JC, Lee JC, Lees CW, *et al*. Genome-wide association study of ulcerative colitis identifies three new susceptibility loci, including the HNF4A region. *Nat Genet* 2009;41:1330–4.
13 Thompson AI, Lees CW. Genetics of ulcerative colitis. *Inflamm Bowel Dis* 2011;17:831–48.
14 Peters U, Jiao S, Schumacher FR, *et al*. Identification of Genetic Susceptibility Loci for Colorectal Tumors in a Genome-Wide Meta-analysis. *Gastroenterology* 2013;144:799–807.e24.
15 Fine JD, Mellerio JE. Extracutaneous manifestations and complications of inherited epidermolysis bullosa: part I. Epithelial associated tissues. *J Am Acad Dermatol* 2009;61:367–84; quiz 385–6.
16 Huang BL, Chandra S, Shih DQ. Skin manifestations of inflammatory bowel disease. *Front Physiol* 2012;3:13.
17 Niculescu C, Ganguli-Indra G, Pfister V, *et al*. Conditional ablation of integrin alpha-6 in mouse epidermis leads to skin fragility and inflammation. *Eur J Cell Biol* 2011;90:270–7.
18 el Marjou F, Janssen KP, Chang BH, *et al*. Tissue-specific and inducible Cre-mediated recombination in the gut epithelium. *Genesis* 2004;39:186–93.
19 Dowling J, Yu QC, Fuchs E. Beta4 integrin is required for hemidesmosome formation, cell adhesion and cell survival. *J Cell Biol* 1996;134:559–72.
20 Georges-Labouesse E, Messaddeq N, Yehia G, *et al*. Absence of integrin alpha 6 leads to epidermolysis bullosa and neonatal death in mice. *Nat Genet* 1996;13:370–3.
21 van der Neut R, Krimpenfort P, Calafat J, *et al*. Epithelial detachment due to absence of hemidesmosomes in integrin beta 4 null mice. *Nat Genet* 1996;13:366–9.
22 Raul F, Simon P, Kedinger M, *et al*. Intestinal enzymes activities in isolated villus and crypt cells during postnatal development of the rat. *Cell Tissue Res* 1977;176:167–78.
23 Toedter G, Li K, Sague S, *et al*. Genes associated with intestinal permeability in ulcerative colitis: changes in expression following infliximab therapy. *Inflamm Bowel Dis* 2012;18:1399–410.
24 Mombaerts P, Iacomini J, Johnson RS, *et al*. RAG-1-deficient mice have no mature B and T lymphocytes. *Cell* 1992;68:869–77.
25 Tourneur E, Chassin C. Neonatal immune adaptation of the gut and its role during infections. *Clin Dev Immunol* 2013;2013:270301.
26 Sheng YH, Hasnain SZ, Florin TH, *et al*. Mucins in inflammatory bowel diseases and colorectal cancer. *J Gastroenterol Hepatol* 2012;27:28–38.
27 Nowarski R, Jackson R, Gagliani N, *et al*. Epithelial IL-18 Equilibrium Controls Barrier Function in Colitis. *Cell* 2015;163:1444–56.
28 Toivola DM, Krishnan S, Binder HJ, *et al*. Keratins modulate colonocyte electrolyte transport via protein mistargeting. *J Cell Biol* 2004;164:911–21.
29 Johansson ME, Gustafsson JK, Holmén-Larsson J, *et al*. Bacteria penetrate the normally impenetrable inner colon mucus layer in both murine colitis models and patients with ulcerative colitis. *Gut* 2014; 63:281–91.
30 Larmonier CB, Laubitz D, Hill FM, *et al*. Reduced colonic microbial diversity is associated with colitis in NHE3-deficient mice. *Am J Physiol Gastrointest Liver Physiol* 2013;305:G667–77.
31 Xiao F, Yu Q, Li J, *et al*. Slc26a3 deficiency is associated with loss of colonic HCO3 (-) secretion, absence of a firm mucus layer and barrier impairment in mice. *Acta Physiol (Oxf)* 2014;211:161–75.
32 Vaishnava S, Yamamoto M, Severson KM, *et al*. The antibacterial lectin RegIIIgamma promotes the spatial segregation of microbiota and host in the intestine. *Science* 2011;334:255–8.
33 Kanneganti M, Mino-Kenudson M, Mizoguchi E. Animal models of colitis-associated carcinogenesis. *J Biomed Biotechnol* 2011;2011:342637.
34 Miyazaki K. Laminin-5 (laminin-332): Unique biological activity and role in tumor growth and invasion. *Cancer Sci* 2006;97:91–8.
35 Said AH, Raufman JP, Xie G. The role of matrix metalloproteinases in colorectal cancer. *Cancers (Basel)* 2014;6:366–75.
36 West NR, McCuaig S, Franchini F, *et al*. Emerging cytokine networks in colorectal cancer. *Nat Rev Immunol* 2015;15:615–29.
37 Rodius S, Indra G, Thibault C, *et al*. Loss of alpha6 integrins in keratinocytes leads to an increase in TGFbeta and AP1 signaling and in expression of differentiation genes. *J Cell Physiol* 2007;212:439–49.
38 Giancotti FG. Targeting integrin beta4 for cancer and anti-angiogenic therapy. *Trends Pharmacol Sci* 2007;28:506–11.
39 Jones RG, Li X, Gray PD, *et al*. Conditional deletion of beta1 integrins in the intestinal epithelium causes a loss of Hedgehog expression, intestinal hyperplasia, and early postnatal lethality. *J Cell Biol* 2006;175:505–14.
40 Ussar S, Moser M, Widmaier M, *et al*. Loss of Kindlin-1 causes skin atrophy and lethal neonatal intestinal epithelial dysfunction. *PLoS Genet* 2008;4:e1000289.
41 Lachaux A, Bouvier R, Loras-Duclaux I, *et al*. Isolated deficient alpha6beta4 integrin expression in the gut associated with intractable diarrhea. *J Pediatr Gastroenterol Nutr* 1999;29:395–401.
42 Zhang Y, Li W, Li L, *et al*. Structural damage in the *C. elegans* epidermis causes release of STA-2 and induction of an innate immune response. *Immunity* 2015;42:309–20.
43 Fu J, Wei B, Wen T, *et al*. Loss of intestinal core 1-derived O-glycans causes spontaneous colitis in mice. *J Clin Invest* 2011;121:1657–66.
44 Specian RD, Neutra MR. Cytoskeleton of intestinal goblet cells in rabbit and monkey. The theca. *Gastroenterology* 1984;87:1313–25.
45 Huber S, Gagliani N, Zenewicz LA, *et al*. IL-22BP is regulated by the inflammasome and modulates tumorigenesis in the intestine. *Nature* 2012;491:259–63.
46 Kirchberger S, Royston DJ, Boulard O, *et al*. Innate lymphoid cells sustain colon cancer through production of interleukin-22 in a mouse model. *J Exp Med* 2013;210:917–31.
47 Liu J, Duan Y, Cheng X, *et al*. IL-17 is associated with poor prognosis and promotes angiogenesis via stimulating VEGF production of cancer cells in colorectal carcinoma. *Biochem Biophys Res Commun* 2011;407:348–54.
48 Baribault H, Penner J, Iozzo RV, *et al*. Colorectal hyperplasia and inflammation in keratin 8-deficient FVB/N mice. *Genes Dev* 1994;8:2964–73.
49 Habtezion A, Toivola DM, Butcher EC, *et al*. Keratin-8-deficient mice develop chronic spontaneous Th2 colitis amenable to antibiotic treatment. *J Cell Sci* 2005;118:1971–80.
50 Habtezion A, Toivola DM, Asghar MN, *et al*. Absence of keratin 8 confers a paradoxical microflora-dependent resistance to apoptosis in the colon. *Proc Natl Acad Sci USA* 2011;108:1445–50.
51 Guo W, Pylayeva Y, Pepe A, *et al*. Beta 4 integrin amplifies ErbB2 signaling to promote mammary tumorigenesis. *Cell* 2006;126:489–502.
52 Stewart RL, O'Connor KL. Clinical significance of the integrin $\alpha 6\beta 4$ in human malignancies. *Lab Invest* 2015;95:976–86.
53 Raymond K, Kreft M, Song JY, *et al*. Dual Role of alpha6beta4 integrin in epidermal tumor growth: tumor-suppressive versus tumor-promoting function. *Mol Biol Cell* 2007;18:4210–21.
54 Zhang H, Landmann F, Zahreddine H, *et al*. A tension-induced mechanotransduction pathway promotes epithelial morphogenesis. *Nature* 2011;471:99–103.

GUT

Hemidesmosome integrity protects the colon against colitis and colorectal cancer

Adèle De Arcangelis, Hussein Hamade, Fabien Alpy, Sylvain Normand, Emilie Bruyère, Olivier Lefebvre, Agnès Méchine-Neuville, Stéphanie Siebert, Véronique Pfister, Patricia Lepage, Patrice Laquerriere, Doulaye Dembele, Anne Delanoye-Crespin, Sophie Rodius, Sylvie Robine, Michèle Kedinger, Isabelle Van Seuningen, Patricia Simon-Assmann, Mathias Chamaillard, Michel Labouesse and Elisabeth Georges-Labouesse

Gut 2017 66: 1748-1760 originally published online July 1, 2016
doi: 10.1136/gutjnl-2015-310847